On RF Material Characterization in the Stripline Cavity

Claude M. Weil, *Fellow, IEEE*, Chriss A. Jones, Yehuda Kantor, and John H. Grosvenor, Jr.

***Abstract*—We examine the accuracy of the air-filled stripline cavity in measuring the dielectric and magnetic properties of bulk materials in the frequency range of 150–2000 MHz. Measured data on complex permittivity and permeability for several different-sized specimens of dielectric and magnetic materials were compared with reference values obtained using other techniques of known uncertainties. Major differences were noted for both complex permittivity and permeability data, and we largely attribute these to less-than-optimal perturbation of the internal cavity fields by the material specimens under test. The technique is particularly unsuited to measuring the dielectric loss of the higher-permittivity low-loss materials due to energy scatter by the specimen under test. In order to improve measurement accuracy, we suggest guidelines on the range of specimen electric and magnetic volume needed for optimal cavity perturbation.**

***Index Terms*—Cavity, dielectric, ferrite, loss factor, magnetic, materials, measurements, permeability, permittivity, radio frequency, resonator, stripline.**

I. Introduction

TECHNIQUES for measuring the dielectric and magnetic properties of bulk materials at RF/microwave frequencies can generally be divided into two basic categories: broad-band transmission-line methods, such as the coaxial air line technique, for medium- to high-loss materials, and high-Q cavity resonator methods for low-loss materials. Many different resonator techniques are available, but few of these can operate in the critical VHF/UHF (30–3000 MHz) frequency range of the electromagnetic spectrum due to the very large physical size of such structures. One of the resonator techniques capable of operating in this frequency range is the air-filled stripline cavity.

Historically, this technique was developed in the early 1960's by Waldron and Maxwell [1]–[4] to measure the permeability of demagnetized ferrites in this frequency range. At frequencies below gyromagnetic resonance (1–1000 MHz), most ferrites exhibit strong magnetic properties with medium- to high-magnetic loss factors. The technique is one of a class of cavity methods, developed four to five decades ago, which rely on small-perturbation theory for the derivation of the material parameters (see, e.g., [5]). Due to the small specimen sizes used and the correspondingly low cavity filling factors that result, these methods work well for materials that possess a wide range of dielectric and magnetic losses. The method has been widely implemented in U.S. industrial and government laboratories, and stripline cavity fixtures are commercially available from a U.S. manufacturer in both untunable (fixed length) and tunable (variable length) versions [6].

When compared to other techniques, the stripline cavity possesses some significant advantages and disadvantages. One of its major advantages is that, in contrast to most other resonator techniques, the unit is capable of multifrequency operation over a wide frequency range, using up to ten or more harmonics of the unit's fundamental resonance. Another advantage is that the resonator has a uniaxial or very nearly uniaxial field structure. This allows for measurements of anisotropic materials by orienting the specimen under test either parallel or normal to the E- or H-fields of the resonator. Such measurements are not possible in the coaxial air line, due to its radial field configuration. Other advantages include the capability to measure small samples of high-loss magnetic films, as well as the reduced cost of specimen preparation (rectangular shape versus very accurately machined toroid), as discussed by Waldron [1]. In addition, specimens under test can be readily introduced through the open sides of the structure. The most significant disadvantage is that the method is incapable of satisfactorily resolving the highly dispersive (frequency-dependent) permeability properties of ferrites in the VHF/UHF frequency range due to the cavity's inadequate low-frequency limit and its poor frequency resolution (the resolution problem is avoided in tunable resonators). As already mentioned, the technique relies on small-perturbation theory for the derivation of material parameters. Since such techniques are known to be very susceptible to measurement error, this constitutes another potential disadvantage.

A stripline cavity fixture was designed and fabricated at the National Institute of Standards and Technology (NIST), Boulder, CO [7] for purposes of assessing the quality of this measurement technique as well as to provide NIST with a capability for participating in a NIST-organized intercomparison of stripline cavity measurements [8]. We report here on complex permittivity and permeability measurements of several different materials. We compare these measurement data with reference data obtained using other techniques, primarily the coaxial air line method [9], and summarize the differences seen in the data. In this study, we attempted to address three significant questions. First—is the method's reliance on small-perturbation theory for the derivation of material parameters [5] a significant source of measurement inaccuracy? Second—does the method reliably measure the loss factor of low-loss dielectrics? Third—how susceptible is this technique to air-gap errors (a major source of inaccuracy in many measurement techniques)?

Manuscript received December 14, 1998.

C. M. Weil, C. A. Jones, and J. H. Grosvenor, Jr., are with the Radio-Frequency Technology Division (813.01), National Institute of Standards and Technology, Boulder, CO 80303-3328 USA.

Y. Kantor is with the Electric Systems Division, Department 87, RAFAEL, Haifa, Israel.

Publisher Item Identifier S 0018-9480(00)00846-2.

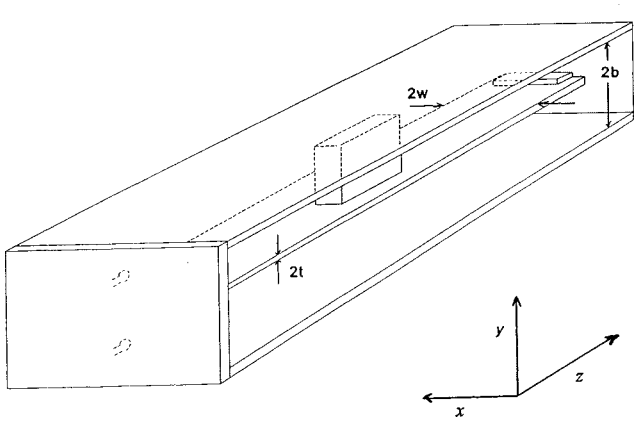

Fig. 1. Stripline cavity showing required specimen locations for measurement of complex permittivity (axial mid-point) and complex permeability (adjacent to end plate).

If it is more prone than comparable techniques, then this clearly constitutes a further disadvantage.

II. Experimental Methodology

A. General Description

The stripline cavity is illustrated in Fig. 1. It consists of a center-strip conductor mounted equidistantly between two ground planes and terminated by two end plates. Generally, the end plates are permanently attached to the ground planes, thus, the resonator is of fixed length and untunable. In a few cases, tunability is achieved by including a capability to adjust the axial position of one end plate. Such an advantage is gained at the cost of greatly increased mechanical complexity and potential electrical contact problems that can lead to reduced cavity quality (Q) factor.

A propagating TEM mode is excited within the stripline structure using either coupling loops mounted in one of the end plates or a monopole probe mounted in the ground planes and adjustable in axial position. The first or fundamental resonance is achieved when the resonator length corresponds to a half-guide wavelength of the exciting frequency. Additional resonances will occur at harmonic frequencies of the fundamental, assuming that the length remains unchanged. Two-port resonators, containing two coupling loops or monopole probes mounted on both sides of the center strip, allow for transmission factor measurements, which usually provide for more accurate cavity modal parameter measurements than does a one-port resonator. The Waldron perturbation theory [1] dictates that the dielectric parameters are derivable only when the magnetic-field (H-field) intensity is zero and that, similarly, the magnetic parameters are derivable only when the electric-field (E-field) intensity is zero. Consequently, complex dielectric permittivity ($\varepsilon^* = \varepsilon' - j\varepsilon''$) measurements are performed by placing the specimen at an axial H-field node of the resonator. For the case of fundamental and odd-harmonic resonances, the H-field node occurs at the axial midpoint of the structure (see Fig. 1). For even-harmonic resonances, the test specimen needs to be axially moved to a new H-field node location. Similarly, measurements of the complex magnetic permeability ($\mu^* = \mu' - j\mu''$) are conducted by placing the specimen under test at an axial E-field node, located at the structure's end plates (see Fig. 1). The manner in which permeability measurements for ferrite specimens are usually conducted is illustrated in more detail in Fig. 2 (see [1, Case 3]). When the material is magnetically anisotropic, other specimen orientations are used, in order to measure the other two components of the permeability tensor (see [7, Cases 1 and 2]). The finite sample width that straddles the field nodes during measurements is a cause of small, but not significant error.

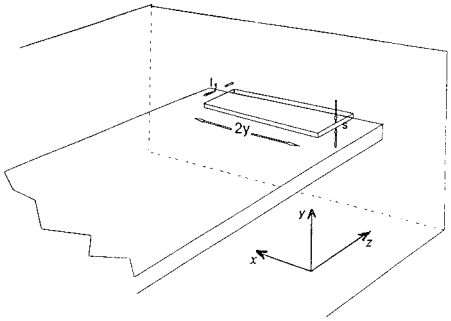

Fig. 2. Usual placement of magnetic specimen for measurement of the x-component of complex permeability (corresponds to Waldron's Case 3 [1]).

B. Design and Fabrication of the NIST Fixtures

The dimensional design of the stripline cross section critically affects the accuracy with which materials can be characterized, particularly for dielectric materials. The design needs to be one in which the electric and magnetic fields are as uniform as possible within the specimens under test. Maximizing the ratio w/b (see Fig. 1) leads to minimal E- and H-field nonuniformity. However, this also increases the conductor losses, which results in a lower resonator Q-factor. This, in turn, reduces the fixture's sensitivity for measuring dielectric and magnetic loss factors of low-loss materials. Since these criteria clearly work in opposition, a compromise must be chosen between the requirements of good field uniformity and adequate quality factor.

Waldron [1], [3] predicted the electromagnetic fields within the stripline geometry by transforming the known fields of a parallel-plate structure to this structure using the modified Schwartz–Christoffel transformation. He developed three basic expressions that define the critical cross-sectional dimensions b, t, and w in terms of two dimensionless parameters $\alpha > 1$ and $\beta < 1$ relating to the E-field uniformity between the center strip and ground planes. The closer the parameters α and β approach one, the more uniform the E-field becomes. Waldron [1] also included two design plots showing the variation of t/b and w/b versus $\alpha - 1$ for different values of the parameter $\sin^{-1}\beta$, ranging from 75° to 89°; loci curves of constant nonuniformity error are also included in these plots. Jones [7] has recently reviewed these equations and design plots, and they are not repeated here.

The length of our fixture was selected as $l_0 = 1$ m (39.37 in), giving a fundamental resonance of approximately 150 MHz with harmonic resonances spaced at 150-MHz increments above the fundamental. The resonator's upper frequency limit is defined by the frequency at which the first higher

order TE_{10} mode begins to propagate in the stripline. For the open-sided structure, this occurs when the ground plane separation $2b = \lambda/2$, assuming lossless conductors. We chose a value of $2b = 76.2$ mm (3 in) for the ground plane separation, giving a theoretical upper frequency limit of 1970 MHz. In setting our cross-sectional dimensions for the line, we chose a compromise goal of 0.5% for the field nonuniformity error. Using the Waldron design plots, we chose α to be 1.0067 and $\sin^{-1}\beta$ to be 85.6°. The ratio w/b was then read off as 1.333 and the ratio t/b as 0.167. The remaining design parameters were then computed as follows: center strip width $2w = 101.6$ mm (4 in), center strip thickness, $2t = 12.7$ mm (0.5 in).

We constructed two fixtures, each having the same cross-sectional dimensions and length, but of different ground plane widths and thicknesses. These were vertically suspended in a steel frame in order to ensure that the structure was not distorted by gravity. Using the criterion suggested by Collin [10], that the ground-plane width be three times the separation in order to keep leakage of RF energy through the open sides to a practical minimum, we chose the ground plane dimensions for the first unit to be 305-mm (12 in) wide and 6.35-mm (0.25 in) thick. However, during permittivity measurements, we noted that placing a conductive object at the open sides of the cavity significantly affected the measured cavity Q-factor, particularly at the higher frequencies. We attributed this effect to energy scattered by the sample under test. This unit also lacked sufficient structural rigidity, resulting in potential loss of parallelism. In efforts to resolve both these problems, we constructed a second fixture with wider 635-mm (25 in) and thicker 12.7-mm (0.5 in) ground planes. In order to keep the structural weight within practical limits, the second unit was constructed of MIC6 aluminum, as opposed to the OFHC copper used in the first. During assembly of both units, a conductive paste was applied to all fixture joints in order to improve the electrical continuity of the structure.

Small diameter loops mounted in the end plates (see Fig. 1), which couple into the TEM mode magnetic fields, were used to excite the cavity, rather than the monopole probes used by Waldron and Maxwell [1], [2].

C. Material Measurement Techniques

Before attempting any material measurements, we characterized the empty resonator by measuring its loaded Q-factor. These data were compared to theoretical predictions (see Section III).

For this study, we selected six separate materials that are commercially available from the U.S. electronics material industry. The properties of these materials have been extensively measured at NIST. They included two dielectrics, cross-linked polystyrene (CPS) and alumina plus four ferrites, a ferrite-loaded polymer (FLP), a nickel ferrite (Ni), a nickel–zinc ferrite (Ni–Zn), and an yttrium–iron garnet (YIG). We measured both dielectric and magnetic properties of the FLP and YIG. As in all material characterization measurement performed in a cavity resonator, the real parts ε_r' and μ_r', of the complex permittivity and permeability are derived from measurements of the shift Δf in resonant frequency for the resonator plus specimen, relative to that of the empty resonator f_0. Likewise, the imaginary parts ε_r'' and μ_r'' are derived from the change in the measured resonator Q-factor for the resonator plus specimen Q_1 relative to that for the empty resonator Q_0. Almost all data on complex permittivity and permeability were derived using Waldron's small perturbation theory [1].

1) Permittivity Measurements: For dielectric-property measurements, the rectangular specimen under test needs to have a width along the y-axis (see Fig. 1) that covers the full distance b–t between center strip and ground plane in order to minimize dielectric depolarization errors. The slab is located in the region of maximum and uniaxial E-field, specifically at the midpoint, $x = 0$, of the center strip, and with the smallest dimension oriented along the x-axis in order to minimize the E-field nonuniformity across the specimen. In order to avoid potential measurement error caused by the need to relocate the specimen to different axial positions, we kept the dielectric specimens at the axial mid-point of the cavity and conducted measurements at the fundamental and odd-harmonic resonances only.

During permittivity measurements, we discovered empirically that scattered energy losses could be reduced considerably by mounting identical specimens of the same material under test on both sides of the center strip (i.e., symmetrically loading the cavity). Most of the complex permittivity data, given in the following section, were derived in this way, based on the assumption that measured values of Δf and $1/Q_1 - 1/Q_0$ are double what they would be for a single specimen; i.e., $\Delta f_S = 2\Delta f_U$ where the subscripts denote symmetric and unsymmetric loading, respectively.

In deriving his small perturbation theory for permittivity, Waldron [1] chose a thin rectangular slab for his specimen shape, with dimensions as follows (see Fig. 1): $2y$ in the x-direction, b–t in the y-direction, and $2l_1$ in the z-direction. Although somewhat confusing, Waldron's original symbols are retained in this paper in order to simplify the application of Waldron's perturbation formulas. Using Waldron's equation [1, eq. (55)] (there appear to be errors in this), we derived the following expressions for ε_r'' and ε_r':

$$\varepsilon_r' = 1 + \frac{\Delta f}{f_0}\,\frac{bl_0}{2Ayl_1} \tag{1a}$$

$$\varepsilon_r'' = \left(\frac{1}{Q_L} - \frac{1}{Q_0}\right)\,\frac{bl_0}{4Ayl_1} \tag{1b}$$

where l_0 is the cavity length, s is the half of the ground plane separation, and A is the geometrical factor given by

$$A = \frac{\pi\alpha}{2(\alpha+\beta)K(1/\alpha)}\sqrt{\frac{\alpha^2+\beta^2}{\alpha^2-1}}\,. \tag{2}$$

The parameters α and β are defined by the resonator dimensions, as discussed above in Section II-B [1], and $K(1/\alpha)$ is the complete elliptic integral of the first kind with modulus $1/\alpha$.

Due to the well-known limitations of small-perturbation theory, we also briefly investigated the application of a commercially available finite-element code to the problem

TABLE I
PHYSICAL DIMENSIONS AND RANGE OF ELECTRICAL VOLUME FOR SPECIMENS USED IN COMPLEX PERMITTIVITY MEASUREMENTS

Spec. No.	Material	$2y$ mm	b-t mm	$2l_1$ mm	Electrical Volume, $4y(b-t)l_1/\lambda^3$ x 10^{-6}	Dielectric Depolarization Correction $\epsilon_c' - \epsilon_m'$
1S	CPS	6.353	31.752	12.749	1.3 to 2900	+0.001
2U		12.729	32.108	25.4	5.2 to 11 706	
3S	Alumina	3.167	31.761	6.378	2.4 to 5100	+0.06
4U		3.174	32.126	12.71	4.8 to 10 303	
5S	FLP	3.131	31.755	6.356	5.1 to 10 700	+0.17
6U		3.172	31.471	12.71	10.2 to 21 483	
7S	YIG	3.185	31.752	6.356	5 to 11 000	+0.17

of the stripline cavity containing a dielectric sample [11]. In this very preliminary numerical study, one-quarter of the cavity-plus-sample was modeled using perfect electric and magnetic conductive boundaries at the planes of symmetry. Using an assumed ε_r' value for the dielectric sample, the inside volume was subdivided into about 6700 hexahedrons. The code then predicted the resonant frequency shift Δf, which was compared to the measured value. An "inverse" code, capable of predicting ε_r' values from measured Δf values for this cavity, was not available to us.

Table I lists the various specimens used in the complex permittivity measurements. S or U, shown next to the specimen number in column 1, designates whether the measurement involved symmetrical or unsymmetrical loading of the cavity. In order to study the influence of size on measurement accuracy, two different sized specimens of CPS, alumina, and FLP were used. Specimen dimensions are listed in the following three columns; for the case of symmetrical loading, the data given represent an average of the two samples measured. Column 6 lists the range of the specimen's electric volume $4y(b-t)l_1/\lambda^3$, where λ is the wavelength within the material under test, for the lowest to highest frequency. These data relate to how much the specimen perturbs the cavity fields and are discussed further in Section IV. The last column of Table I lists the dielectric depolarization correction in ε' caused by the presence of air gaps. This is further discussed in Section II-D.

2) Permeability Measurements: For magnetic characterization, measurements were only performed as shown in Fig. 2, corresponding to Waldron's Case 3 [1]. For these measurements, the need to ensure minimal H-field nonuniformity across the specimen and the critical need to minimize the magnetic depolarization error dictates use of long and thin rectangular specimen shapes. The single specimen is located in a region of maximum and uniaxial H-fields; i.e., on the center strip and flush against the cavity end plate. This allows for measurements at both the odd- and even-harmonic resonances. Energy leakage was generally not a problem during magnetic measurements so that only unbalanced measurements were performed.

In deriving his small-perturbation theory for permeability, Waldron [1] again chose a thin rectangular slab with dimensions as follows (see Fig. 2): $2y$ in the x-direction, s in the y-direction, and l_1 in the z-direction. Using Waldron's equation [1, eq. (60)], we derived the following expressions for μ_r' and μ_r'':

$$\mu_r' = 1 + \frac{\Delta f}{f_0} \cdot \frac{b(b-t)l_0}{Bysl_1} \tag{3a}$$

$$\mu_r'' = \left(\frac{1}{Q_L} - \frac{1}{Q_0}\right) \cdot \frac{b(b-t)l_0}{2Bysl_1} \tag{3b}$$

where B is also a geometrical factor given by

$$B = \frac{A}{2}\left(1 + \frac{\beta}{\alpha}\right). \tag{4}$$

Table II lists the various specimens used in the complex permeability measurements. Since we were again interested in studying the influence of size on measurement accuracy, two different-sized specimens of FLP were used. Specimen dimensions are listed in Columns 3–5. Column 6 similarly lists the range of the specimen's magnetic volume $2ysl_1/\lambda^3$ from its minimum value at 150 MHz to its maximum value (For Ni–Zn and YIG, the peak magnetic volume occurs at frequencies much below 1950 MHz and are given in Column 6.) The last column of Table II lists the demagnetization correction D. This is also discussed further in the following subsection.

D. Dielectric and Magnetic Depolarization Errors

Air gaps are frequently a major source of error in material property measurements. Depolarization errors occur whenever a normal component of the E- or H-field exists at the air–material interface. Since the normal component of electric or magnetic flux density must be continuous at the air–material interface, a discontinuity in the normal E- or H-fields results owing to the differences in ε^* and μ^* for the material and air. The resulting depolarization error always causes measured permittivity or permeability data to be biased lower than actual values and can usually be corrected for by using models, some of which are simple and others more sophisticated. The depolarization problem exists for both dielectric and magnetic measurements in the stripline resonator.

For dielectric measurements, there exist small, but finite air gaps between both x–z specimen faces and the lower and upper conductors (see Fig. 1). This creates a discontinuity in the normal y-directed component of the E-field. The computed

TABLE II
PHYSICAL DIMENSIONS AND RANGE OF MAGNETIC VOLUME FOR SPECIMENS USED IN COMPLEX PERMEABILITY MEASUREMENTS

Spec. No.	Material	$2y$, mm	s, mm	l_1, mm	Magnetic Volume, $2ysl_1/\lambda^3$ x 10^{-6}	Demagnetization Correction, D
8	FLP	38.123	3.119	6.302	0.86 to 1200	0.06611
9		70.129	3.185	9.990	2.57 to 3573	0.03752
10	Ni Ferrite	50.848	1.601	3.206	0.23 to 160	0.01655
11	Ni-Zn Ferrite	42.470	1.030	4.000	1.74 to 7.5 (at 1050 MHz)	0.01715
12	YIG	50.900	1.597	3.193	2.31 to 10.8 (at 600 MHz)	0.01644

dielectric depolarization correction, listed in the last column of Table I, was derived using a simple frequency-independent correction model. This consists of three parallel-plate capacitors in series, following the model developed by Baker–Jarvis for the coaxial air line geometry (see [9, pp. 101–103]); fringing fields were ignored. The corrected value of relative permittivity (real part) ε_c' is related to measured value ε_m' as follows:

$$\varepsilon_c' = \frac{\varepsilon_m'\Big[(b-t)-2g\Big]}{(b-t)-2g\varepsilon_m'} \tag{5}$$

where b and t are cavity dimensions, defined earlier, and g is the air-gap dimension, assuming identical gaps above and below the specimen of 0.025 mm (0.1 mil). The corrections shown in Table I are based on measured permittivity ε_m' data obtained in the cavity and are seen to range from an insignificant +0.001 (0.04%) for CPS ($\varepsilon_m' = 2.5$) to +0.17 (1.1%) for the two ferrites listed ($\varepsilon_m' = 15.8$ for both).

Magnetic depolarization will occur in any TEM mode structure, where the material specimen under test does not completely surround the inner conductor [2], [12]–[14]. For the stripline cavity, a serious discontinuity in the normal x-directed component of the H-field clearly exists at the two y–z end faces of the specimen. This effect can be minimized by reducing the cross-sectional area of the specimen end faces as much as practical. It is also essential to apply a depolarization correction to measured data. Waldron and Maxwell [12] first recognized the need for this correction. Musal [13] subsequently derived an expression giving the corrected value of complex permeability μ_c^* in terms of a measured value μ_m^* and a dimensionless parameter termed the "demagnetization factor" D

$$(\mu_c^* - 1) = \frac{(\mu_m^* - 1)}{1 - D(\mu_m^* - 1)} \tag{6}$$

where

$$D = \frac{syl_1}{4}\int_0^\infty \frac{dx}{(y^2+x)\sqrt{(s^2+x)(l_1^2+x)(y^2+x)}} \tag{7}$$

for the case where the magnetic field is directed along the x-axis, as shown in Fig. 2. If the rectangular specimen shape is represented by a long prolate ellipsoid of aspect ratio in the range of 10–40, approximate solutions to (7) can be obtained using classical expressions derived by Stoner [15]. However, we were able to derive more accurate values for (7) based on the specimen dimensions used, by means of a well-known mathematical package [16]. The values of D are listed in the last column of Table II. Equation (6) was separated into real and imaginary components, which allowed for both μ_r' and μ_r'' to be independently corrected. Although the values of D are small, the correction significantly increases measured permeability values and was greatest for the Ni–Zn ferrite and the YIG, which exhibit substantial permeability values at the lowest measurement frequency; namely, 150 MHz. The correction increased measured values for the YIG at 150 MHz by +3.52 (+25.1%) and +7.27 (+33.8%) for the nickel–zinc ferrite. These corrections clearly cannot be ignored.

III. MEASUREMENT RESULTS

A. Q-Factor of Empty Cavity

Data on the measured and predicted loaded Q-factor versus frequency for the NIST cavity (copper version) are shown in Fig. 3; measured values range from approximately 4000 at fundamental resonance to approximately 12 000 at the upper frequency limit. Since the coupling factor for the small excitation loops is of the order of about –26 dB at 150 MHz, the theoretical loaded and unloaded Q-factors may be assumed to be identical. The large differences seen in Fig. 3 between measured and predicted data can be accounted for by energy losses due to finite RF metal conductivity plus leakage from the open sides of the unperturbed cavity, which were not accounted for. Only the difference in measured Q-factors is used in deriving material loss factors values.

B. Comparison Data

The reader cannot properly evaluate the quality and accuracy of any materials characterization technique without having reference data against which the technique's measured data can be compared. Such data need to have been generated using other techniques that are known to be equally or more accurate than the stripline resonator method. For CPS and alumina, we relied on NIST resonator data obtained at X-band frequencies and

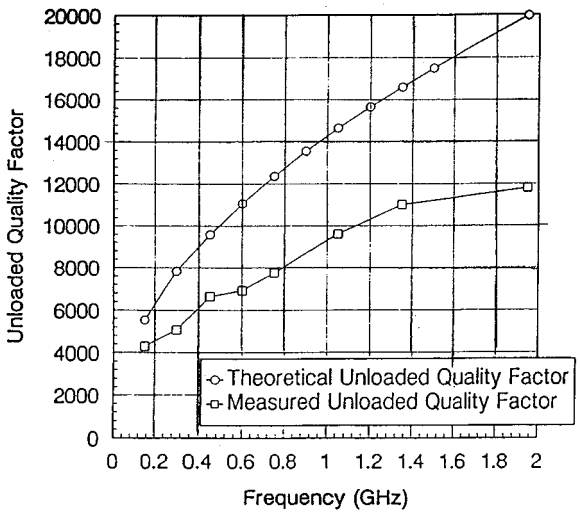

Fig. 3. Measured and predicted quality factors versus frequency for the NIST 1-m-long copper cavity.

accurate to $\pm 0.5\%$ in ε' and $\pm 10^{-4}$ in ε'' (see [17, Tables III and V]; data on CPS are listed in Table III and data on alumina are listed in Table V under "C9"). With the exception of the FLP, all of the materials used for permittivity measurements exhibit little change in their ε_r' values with frequency due to inherently low dielectric loss. The same NIST resonator data [17] show that ε_r' values for both CPS and alumina decrease by about 1.1% for a decade increase in frequency 1–10 GHz. The change in ε_r' values for the YIG was assumed to be the same as that for alumina. For the FLP, which exhibits medium dielectric loss, we relied on NIST data obtained with the 7-mm coaxial air line technique [18]. Since this technique is very prone to air-gap errors when used for ε' measurements, the measurement uncertainties are normally about $\pm 5\%$ in ε' and ± 0.01 in ε'' [9]. However, a single-frequency measurement performed at 500 MHz using the reentrant cavity technique and accurate to $\pm 2.5\%$ in ε' [18] allowed us to tighten up this uncertainty across the 150–2000-MHz band.

For the magnetic measurements, we relied solely on comparison permeability data obtained with the 7-mm-diameter coaxial air-line technique [18]. This technique is largely unaffected by air gap problems when used for μ^* measurements; in this frequency range, the uncertainties are estimated to be $\pm 1.5\%$ in μ' and $\pm .01$ in μ'' [9]. Based on the results of an extensive intercomparison of ferrite measurements using the 7-mm-diameter coaxial air-line technique, NIST has concluded that this technique is the best available for measuring the permeability of ferrites in the 50–2000-MHz frequency range [18].

Well-known imperfections in manufacturing methods can lead to significant lot-to-lot differences in material property data, particularly for magnetic materials. The coaxial air line or cavity specimens used to generate CPS, FLP, Ni, Ni–Zn, and YIG (μ^*) reference data were all derived from the same manufactured lot as those measured in the stripline cavity. The cavity specimens used to generate alumina and YIG (ε^*) reference data did not come from the same lot. These factors need to be kept in mind when comparing the measured data.

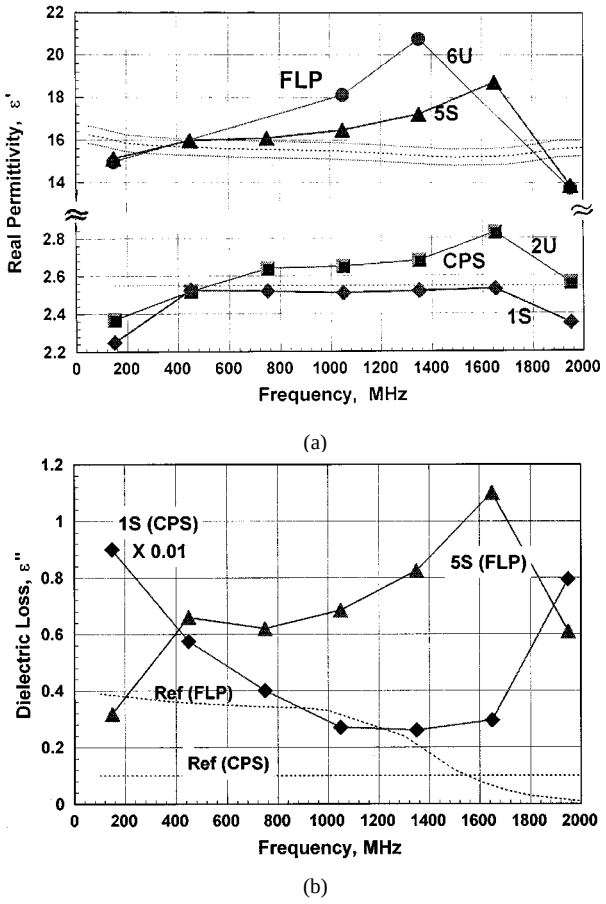

Fig. 4. (a) Measured relative permittivity data for CPS (Specimens 1S and 2U) and FLP (Specimens 5S and 6U). (b) Measured dielectric loss data for CPS (Specimen 1S) and FLP (Specimen 5S).

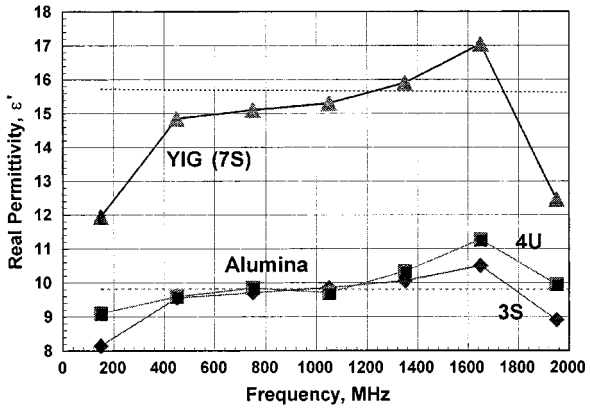

Fig. 5. Measured relative permittivity data for alumina (Specimens 3S and 4U) and YIG (Specimen 7S).

C. Complex Permittivity Data

Measured complex permittivity data for materials listed in Table I are given in Figs. 4 and 5. Reference data, including the estimated uncertainty limits, are shown dotted in both figures. A general observation regarding most of the measured ε^* data shown in Figs. 4 and 5 is that these plots frequently exhibit an almost exponential increase with frequency up to 1650 MHz followed by a significant drop at the last frequency of 1950 MHz. Measurements at 1950 MHz were difficult to perform because

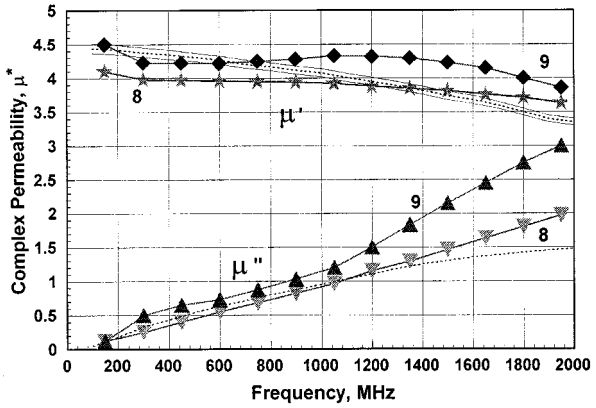

Fig. 6. Measured complex permeability data for FLP (Specimens 8 and 9).

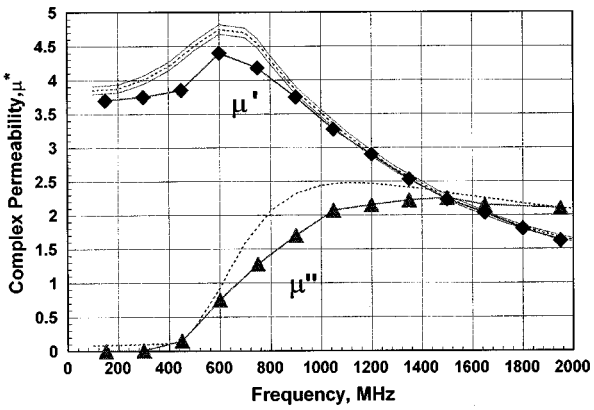

Fig. 7. Measured complex permeability data for Ni Ferrite (Specimen 10).

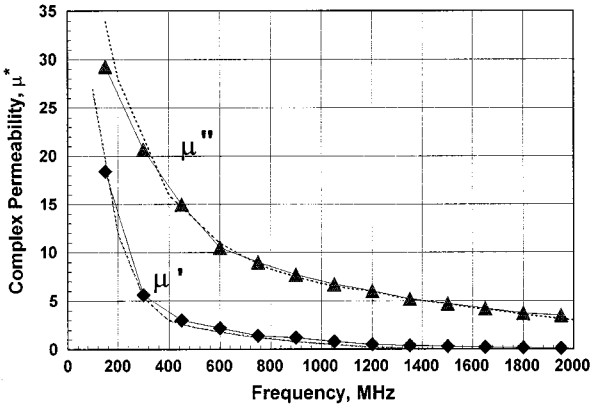

Fig. 8. Measured complex permeability data for Ni–Zn ferrite (Specimen 11).

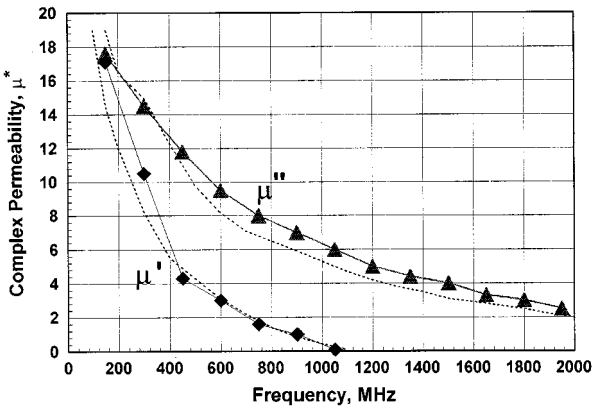

Fig. 9. Measured complex permeability data for YIG (Specimen 12).

the resonance curve was usually highly asymmetric. The reasons for these effects are discussed in Section IV.

Fig. 4(a) shows measured ε' data for CPS and FLP. For CPS, the reference value is $\varepsilon' = 2.55 \pm 0.01$ [17]. Measured data for Specimen 1S agrees with the reference value within approximately 2% over a frequency range of 450–1650 MHz. Data for Specimen 2U, which has four times the volume of 1S, shows better agreement at low frequencies, but the agreement deteriorates significantly at frequencies above 450 MHz. Results for the limited numerical modeling performed at 150 MHz with Specimen 1 (CPS) gave a predicted frequency shift of 45 kHz. The average measured shift for Specimen 1 was about 47 kHz; hence, results were comparable. For the FLP, measured data for Specimens 5S and 6U lie only within the ±2% uncertainty bounds of the reference data at 450 MHz. The limited data available for Specimen 6U, which has twice the volume of Specimen 5S, show that much greater differences are evident compared to those of 5S.

Fig. 4(b) shows dielectric loss data ε'' for the same materials. For CPS, the reference value is $\varepsilon'' = 0.001 \pm 0.0001$ [17]. Measured ε'' data are two-and-one-half to three times the reference value in the frequency range of 750–1650 MHz. Outside this frequency range, much greater disagreements are evident. Similarly, for the FLP, measured ε'' data are about 1.5–10 times the reference data at most frequencies.

Measured ε' data for alumina and YIG are shown in Fig. 5. For alumina, the reference value is 9.8±0.05 [17]. Measured data for both Specimens 3S and 4U agree closely with the reference value at 750 and 1050 MHz. Data for Specimen 4U, which has double the volume of Specimen 3S, show better agreement with the reference value at 150 MHz. Conversely, data for 3S show better agreement than 4U at the higher frequencies, 1350 and 1650 MHz. For the YIG, the reference ε' value is 15.75 ± 0.15 [18]. The measured data for Specimen 7S differ by +7% to –32% relative to the reference value. Measured ε'' data for alumina and YIG were 16 to 50 times reference values. Since these data are clearly meaningless, they are not included here.

D. Complex Permeability Data

Measured complex permeability data for all materials listed in Table II are shown in Figs. 6–9, which shows measured data for the FLP. The μ' data for Specimen 9, which has three times the volume of Specimen 8, is in better agreement with reference values at low frequencies than that for Specimen 8. The converse is true at the highest frequencies, where both μ' and μ'' data for Specimen 8 agree more closely with reference values.

Fig. 7 shows measured data for the Ni ferrite (Specimen 10). The μ' data are about –8% below reference values at the lower frequencies, but agree well above 1200 MHz. With the exception of the lowest and highest frequencies, the μ'' data are about –50% low.

Fig. 8 shows measured data for the Ni–Zn ferrite (Specimen 11). Data for μ' and μ'' agree well with reference

values at most frequencies with some deterioration at the lowest frequencies. Fig. 9 shows measured data for the YIG (Specimen 12). In the mid-frequency range of 600–1100 MHz, μ' data agree within about ±5% of reference values. Below 600 MHz, these data are up to +15% above reference. Data for μ'' are about +20% above reference values over the same frequency range, with better agreement at frequencies below 600 MHz.

IV. Discussion and Conclusions

A. Complex Permittivity Measurements

Figs. 4 and 5 show that measured ε' data were consistently below reference data (by as much as −30%) at the lowest frequency and that the differences are size-dependent; differences were always smaller for the larger volume specimens. We attribute most of these errors to greater uncertainties in the measured resonant frequency shift δf caused by poorer signal-to-noise levels and difficulties in correctly measuring the resonant frequency. We have termed this effect "under-perturbation." Inaccuracy in the air-gap correction also contributes to the total error at this frequency. As frequency is subsequently raised, the measured data exhibit very significant departures from reference values. This error is shown to also be size dependent and is consistently less for the smaller sized specimens at these frequencies. We attribute this error to over-perturbation by the specimen that exceeds the limits of Waldron's theory. The specimen's electrical volume, as given in Table I, provides a useful way of quantifying the degree of cavity perturbation, and is discussed further in Section III-C.

We attribute the sudden drop in ε^* values seen in Figs. 4 and 5 for all materials at 1950 MHz to the presence of the first higher order TE_{10} mode within the specimen. For dielectric measurements, the material under test completely fills the ground plane-to-center strip space, so that the TE_{10} mode can propagate at frequencies below the theoretical limit of 1970 MHz. This problem can only be avoided by reducing the upper frequency limit of the cavity by about 5%.

The results for dielectric loss, discussed in Section III-B, are clearly unacceptable. For a low-permittivity material such as CPS, the cavity appears to have adequate sensitivity to resolve losses of $\varepsilon'' = 0.001$, but the minimum measurement error is still +250%. Note also that measured dielectric loss data for the FLP follow much the same pattern as that for ε', indicating similar perturbation problems. We attribute the general inaccuracy of dielectric loss measurements to unaccountable energy losses scattered by the specimen that escape out of the open cavity sides. This effect appears to be more significant for the high-permittivity low-loss materials. Even though we attempted to reduce scattered energy losses by using two identical specimens, this did not lead to acceptable results in dielectric loss measurements. An obvious solution to this problem is to close off the open sides with conductors, such that the cavity now has the structure of a rectangular coaxial line or TEM "cell" [19]. However, no perturbation theory exists for this structure, so that numerical methods would be needed to derive the dielectric parameters of the materials under test.

B. Complex Permeability Measurements

The principal improvement in the magnetic characterization measurements, relative to the dielectric, is that this technique is able to measure magnetic loss more accurately, though errors of greater than ±50% were recorded in some cases. This is undoubtedly due to the absence of energy scattering problems in the magnetic measurement mode. Errors in μ' data for $\mu' > 1$ varied from −10% to +16%, which is somewhat better than the errors recorded in the ε' data. As discussed earlier, application of the magnetic depolarization correction is essential for accurate results, particularly in the low-frequency region where materials exhibit high permeability.

Size-dependent perturbation problems, which are virtually identical to those that occurred during permittivity measurements, are evident in the FLP data of Fig. 6. There is also evidence of under perturbation in the Ni ferrite data of Fig. 7. There appears to be little evidence of perturbation issues in the Ni–Zn and YIG data of Figs. 8 and 9. As in the case of permittivity measurements, the computed magnetic volume provides a useful way of quantifying the degree of cavity perturbation during permeability measurements. Table II shows that the magnetic volume numbers are generally lower than those used in the dielectric measurements, with the FLP exhibiting the highest values. The measured μ^* data showed no significant drop at 1950 MHz, in the manner that occurred during permittivity measurements. For magnetic measurements, only a small fraction of the ground plane-to-center strip space is filled by the material under test, so that the TE_{10} mode will not propagate in the specimen at frequencies below 1970 MHz.

C. Conclusions

Based on the measurements performed in this study, we conclude that the stripline cavity, in its open-sided configuration, cannot satisfactorily measure the dielectric loss ε'' of materials. With respect to the three remaining material parameters ε', μ', and μ'', we conclude that the technique can measure these parameters to within uncertainties of ±5%, provided that particular attention is paid to the critical issues of optimal perturbation and specimen sizes. For most of the materials measured, we showed that accuracy correlates closely to the degree of electromagnetic perturbation of the cavity as quantified by the specimen's electrical and magnetic volume. Therefore, this should allow us to develop useful guidelines for choosing specimen dimensions based on an optimal range of specimen electrical and magnetic volume. Most of the materials that we characterized have values of ε' and $\mu' < 10$. We suggest that for this class of materials, the optimal range of electrical and magnetic volume is approximately 100×10^{-6} to 500×10^{-6}. For the high-permeability ferrites measured, Ni–Zn and YIG, the optimal range appears to be lower: approximately 1×10^{-6} to 10×10^{-6}. The reasons why the optimal range is different for these materials is unclear at this time.

Our measurement data show that it was generally not possible to obtain accurate characterization measurements over the full 13 : 1 frequency range of our cavity, using only a single specimen. Improved accuracies are realizable by using progressively smaller specimens as the excitation frequency is

raised, beginning with the largest one at the low-frequency end. Depending on the particular material under test, a minimum of three-to-four separate specimens are required, each specifically tailored to cover roughly an octave sub-band of the cavity's frequency coverage and sized according to the optimal criteria suggested above. Measurements of the high-permeability magnetic materials, such as Ni–Zn and YIG, require fewer specimens because measurements are really only needed in the 150–1200-MHz range. Above this frequency, their magnetic properties have essentially disappeared.

Our preliminary numerical study [11] gave encouraging results, but considerably more work is needed to further adapt such codes to this application and to experimentally validate them. Some additional numerical work has been performed to develop "inverse" codes that derive the material properties from cavity resonance parameters in a waveguide cavity geometry [20]. The development of validated numerical codes for this problem should ultimately eliminate the perturbation errors.

Although certain requirements, such as the shape in which a material is supplied or the need for uniaxial fields, may dictate the use of the stripline cavity technique, other techniques are known to be more accurate at comparable frequencies and are, therefore, preferred. These include the broad-band coaxial air-line technique for complex permeability measurements [9] and the coaxial reentrant cavity method for complex permittivity measurements [17].

ACKNOWLEDGMENT

The authors thank D. Gallagher and J. Boyd, Instrument Shops NIST, Boulder, CO, for fixture design and fabrication, B. O'Connor, Colorado Precision Optics, Longmont, CO, for specimen preparation, J. Baker-Jarvis, M. Janezic, and B. Riddle for reference data and helpful discussions, and the manuscript reviewers for many useful suggestions.

REFERENCES

[1] R. A. Waldron, "Theory of a strip-line cavity for measurement of dielectric constants and gyromagnetic—Resonance line-widths," *IEEE Trans. Microwave Theory Tech.*, vol. MTT-12, pp. 123–131, Jan. 1964.

[2] S. Maxwell, "A stripline cavity resonator for measurement of ferrites," *Microwave J.*, vol. 9, pp. 99–102, 1966.

[3] R. A. Waldron, "Theory of the strip-line cavity resonator," *Marconi Rev.*, vol. 27, pp. 30–42, 1964.

[4] S. Maxwell, "Strip-line cavity resonator for measurement of magnetic and dielectric properties of ferrites at low microwave frequencies," *Marconi Rev.*, vol. 27, pp. 22–29, 1964.

[5] *Standard Test Methods for Complex Permittivity (Dielectric Constant) of Solid Electrical Insulating Materials at Microwave Frequencies and Temperatures to 1650 °C*, ASTM Standard D 2520-95, 1998.

[6] *Microwave Measurement Systems Services and Products, Catalog #17*, Damaskos, Inc., Concordville, PA, Jan. 1998.

[7] C. A. Jones, Y. Kantor, J. H. Grosvenor, and M. D. Janezic, "Stripline resonator for electromagnetic measurements of materials," NIST, Boulder, CO, Tech. Note 1505, July 1998.

[8] C. A. Jones, "Permeability and permittivity measurements using stripline resonator cavities: A comparison," *IEEE Trans. Instrum. Meas.*, vol. 48, pp. 843–848, Aug. 1999.

[9] J. R. Baker-Jarvis, M. D. Janezic, J. H. Grosvenor, and R. G. Geyer, "Transmission/reflection and short-circuit line methods for measuring permittivity and permeability," NIST, Boulder, CO, Tech. Note 1355 (revised), Dec. 1993.

[10] R. E. Collin, *Field Theory of Guided Waves*, 2 ed: IEEE Press, 1991.

[11] C. A. Jones, L. Muth, J. Baker-Jarvis, Y. Kantor, J. DeFord, and P. Wallen, "Stripline resonator analysis using finite element codes," in *Abstracts Nat. Radio Sci. Meeting*, CO, Jan. 3–7, 1995.

[12] R. A. Waldron and S. P. Maxwell, "Note on the measurement of material properties by the stripline cavity," *IEEE Trans. Microwave Theory Tech.*, vol. MTT-13, p. 711, Sept. 1965.

[13] H. M. Musal, "Demagnetization effect in strip-line cavity measurements," *IEEE Trans. Magn.*, vol. 28, pp. 3129–3131, May 1992.

[14] S. L. Browning and E. P. Westbrook, "Stripline cavity design for material characterization," in *Proc. AMTA Workshop*, July 1992, pp. 3.1–3.16.

[15] E. C. Stoner, "The demagnetizing factors for ellipsoid," *Philos. Mag. Ser.*, vol. 7, no. 36(263), pp. 803–821, 1945.

[16] Y. Kantor, "Novel approach for demagnetization effect in stripline resonator," unpublished, Jan. 1995.

[17] J. Baker-Jarvis, R. G. Geyer, J. H. Grosvenor, Jr., M. D. Janezic, C. A. Jones, B. F. Riddle, C. M. Weil, and J. Krupka, "Dielectric Characterization of low-loss materials: A comparison of techniques," *IEEE Trans. Dielect. Elect. Insulation*, vol. 5, pp. 571–577, Aug. 1998.

[18] C. M. Weil, M. D. Janezic, and E. J. Vanzura, "Intercomparison of permeability and permittivity measurements using the Transmission/reflection method in 7 and 14 mm coaxial air lines," NIST, Boulder, CO, Tech. Note 1386, Mar. 1997.

[19] M. L. Crawford, "Generation of standard EM fields using TEM transmission line Cells," *IEEE Trans. Electromag. Compat.*, vol. EMC-10, pp. 189–19 5, Nov. 1974.

[20] K. F. Sabet, "A rigorous numerical solution for characterization of low-loss dielectric materials from cavity measurements," EMAG Technol. Inc., Ann Arbor, MI, Dec. 1995.

Claude M. Weil (M'64–SM'95–F'00) was born in Newcastle-on-Tyne, U.K., on June 26, 1937. He received the B.Sc. degree from the University of Birmingham, Birmingham, U.K., in 1959, the M.S.E. degree, from the George Washington University, Washington, D.C., in 1963, and the Ph.D. degree from the University of Pennsylvania, Philadelphia, in 1970, all in electrical engineering.

Prior to 1964, he worked as a Navy Systems and Instrumentation Engineer and also designed microwave components and antennas. From 1971 to 1983, he was with the Environmental Protection Agency's research program on the health effects of RF radiation. From 1983 to 1985, he was with Boeing Military Aircraft Company, where he was involved with radar cross-section (RCS) measurements and analysis. Since 1986, he has been with the Radio-Frequency Technology Division, National Institute of Standards and Technology (NIST), Boulder, CO, where he developed millimeter wave six-port systems and power standards and currently serves as a Senior Project Leader in the NIST Electromagnetic Properties of Materials Program.

Dr. Weil is member of Sigma Xi and a fellow of the IEEE Microwave Theory and Techniques Society (IEEE MTT-S) and the Instrumentation and Measurements Society. He served as general chairman of the 1997 IEEE MTT-S International Microwave Symposium, Denver, CO.

Chriss A. Jones received the B.A. degree in physics and the M.S.E.E. degree from the University of Colorado, Boulder.

Since August 1990, she has been with the National Institute of Standards and Technology, Boulder, CO, where she was initial involved with picosecond-pulse metrology, then with the Electromagnetic Properties of Materials Project, and currently with the Noise Project. While involved with the Materials Project she worked on the development of a stripline cavity, a 77-mm-diameter coaxial transmission line, a 60-GHz Fabry–Perot resonator, and the dielectric measurement of DNA at extremely low frequency (ELF).

Yehuda Kantor was born in Israel, on October 8, 1950. He received the B.S. and M.S. degrees in physics from the Technion University, Haifa, Israel, in 1976 and 1980, respectively.

In 1980, he joined the Electromagnetic Department, Israeli Armaments Institute (RAFAEL), Haifa, Israel, where he was involved with characterizing dielectric and magnetic materials at microwave frequencies, including high temperature measurements. He also designed multilayered absorbing materials (RAM's). From 1985 to 1992, he designed antennas devices, polarizers and radomes, and developed new methods for measuring the dielectric properties of thin integrated-circuit substrates. From February 1993 to January 1995, he spent a sabbatical leave at the National Institute of Standards and Technology (NIST), Boulder, CO (where he continues to closely interact). During his NIST collaboration, he made major contributions in the design of a stripline cavity as well as in how to more accurately measure the properties of magnetic materials using this technique. He also contributed to the design of a 60-GHz Fabry–Perot semiconfocal open resonator for measuring the dielectric properties of laminar material samples. He is currently involved in applying simulation software to the design of radomes, antennas, microstrip and coplanar transmission lines and MCM packaging at RAFAEL, Haifa, Israel.

John H. Grosvenor, Jr. was born in Great Lakes, IL, in 1948. He received two A.A.S. degrees from Thomas Nelson Community College, Hampton, VA, in 1975, and a Certificate of Completion from the Engineering Technician School, NASA, Langley Research Center, Hampton, VA, in 1982.

He served in the Navy during the late 1960's. Since 1982, he has been with the National Institute of Standards and Technology (NIST), Boulder, CO, where, for the past nine years, he has been associated with the Electromagnetic Properties of Materials Project. Prior to joining NIST, he was with NASA and RCA.